Development of Multi-Stage Fracturing System and Wellbore Tractor to Enable Zonal Isolation During Stimulation and EGS Operations in Horizontal Wellbores

Abstract

This paper discusses the progress on a project funded by the DOE Utah FORGE (Frontier Observatory for Research in Geothermal Energy) for the development of a subsurface heat exchanger for Enhanced Geothermal Systems (EGS) using unique casing sleeves cemented in place and are used first as a system for rapid and inexpensive multi-stage stimulations and second to perform conformance control functions at 225 ºC. The proposed sleeves will use a single-sized dissolvable ball to open for fracture stimulation. After stimulation, and once the balls dissolve, the sleeves are open for immediate fluid injection. A separately designed wellbore tractor specific for both fluid detection and valve manipulation is then deployed to detect and control the injection entry points to create an effective EGS through paired horizontal injectors and *open hole* producers. The wells will be connected through multiple networks of induced and natural fractures that can be controlled throughout the field life.

Introduction

Enhanced Geothermal Systems (EGS) comprise of a system that inject water into wells where water travels through the reservoir and harvests heat from the hot rock; then, the resulting hot water is produced to the surface. This paper discusses a new innovative system, called GeoThermOPTIMAL (Figure 1), in support of the DOE Utah FORGE (Figures 2A and 2B) project for the development of an Enhanced Geothermal Systems (EGS). Multi-stage stimulation techniques in horizontal wells have been applied successfully to reduce costs in unconventional oil and gas wells but not in geothermal wells, due to temperature limitations and casing size limitations, which this paper addresses.

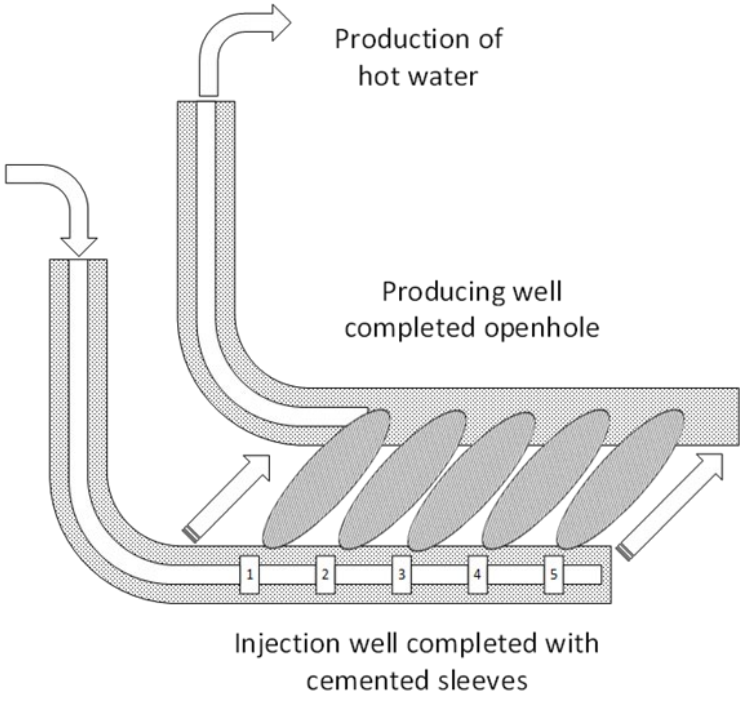

Figure 1: GeoThermOPTIMAL (Fleckenstein et al. 2021)

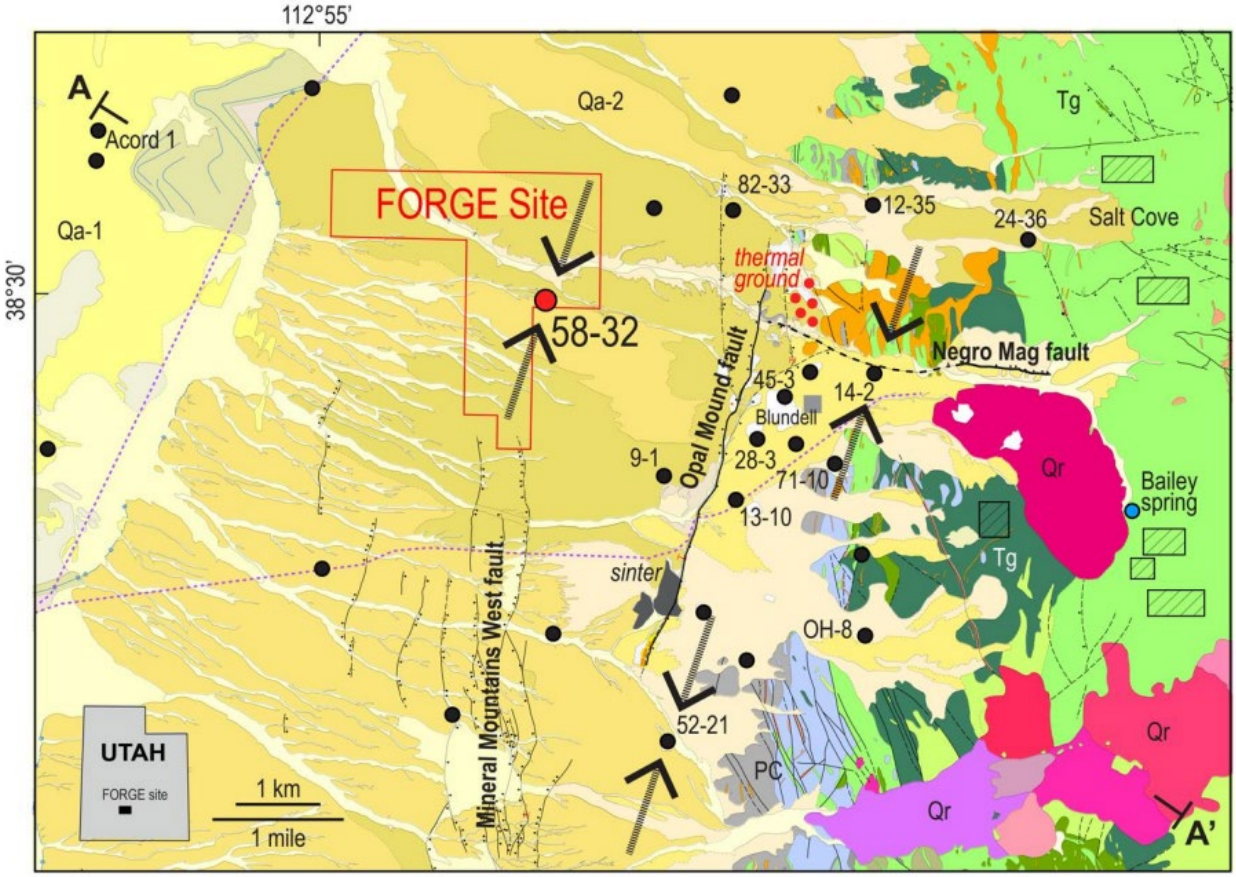

Figure 2-A: Geologic map of the FORGE EGS reservoir site (Simmons et al. 2019)

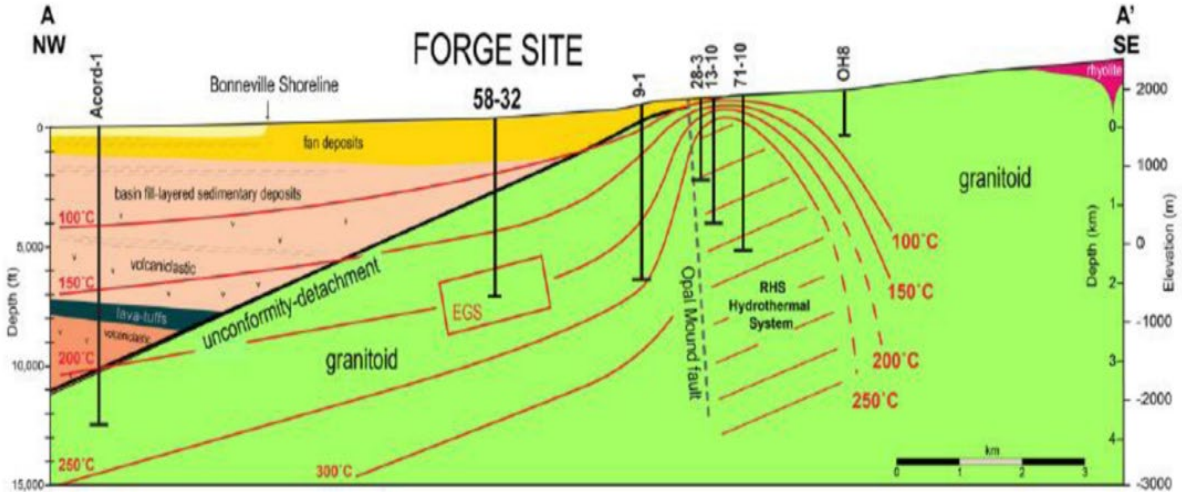

Figure 2-B: FORGE EGS reservoir cross-section. RHS is Roosevelt Hot Springs. (Simmons et al. 2019)

The innovative system uses a unique set of casing sleeves, called FracOPTIMAL sleeves, cemented in place and used both (1) as a system for rapid and inexpensive multi-stage stimulations and (2) to perform conformance control functions at geothermal temperatures of 225 ºC. The sleeves will use a single-sized dissolvable ball to open for a subsequent fracture stimulation. At least two wells will be connected through several networks of induced and natural fractures. After stimulation, and once the balls have dissolved, the sleeves are open for EGS fluid injection. In EGS reservoirs with little natural fracturing, all heat exchange would need to be accomplished through the induced fractures, so the sleeves must be economic

to manufacture, and facilitate rapid and inexpensive multi-stage fracturing operations and then be used for long term conformance control. An advantage of this system would be the use of fresh, or near fresh water as the injection fluid, which will allow the use of low carbon steels in the casing and downhole tools, as well as in the surface equipment and powerplant equipment, instead of expensive corrosion resistant alloys, such as Inconel, which may cost ten times the cost of conventional steels. This will reduce both the initial capital expenditures, and the lack of scaling and corrosion could reduce operating costs. A separately designed wellbore tractor, capable of both fluid detection and valve manipulation, would be deployed to detect and control the injection entry points to create an effective EGS through paired horizontal injectors and open hole producers. Further, the injection fluid would cool the injection wells, allowing more conventional electronic systems to be used in the cooler environment for the detection of fluid flow and avoid the corrosion and scaling tendencies of geothermal waters.

To make an EGS system economic, it has been estimated that the amount of heated fluid necessary to generate 5 MWe (gross) is between 50,000-100,000 barrels per day (bpd). These system design parameters would be dependent on the size of the subsurface heat exchanger that is created, on the temperature of the resource rock, and the heat exchange rates achieved in the system. These rates are a typical per-well generation capacity in the hydrothermal industry and are a good benchmark for an EGS project in today's market (Olson, 2015). The large volume injectors needed for EGS entail the need for larger casing sizes that typically used in shale development, making conventional techniques difficult to shift sleeves in horizontal wells, due to buckling of the small diameter coiled tubing in large diameter horizontal wellbores.

The well performance must be maintained with acceptable heat recovery for 20-30 years. To achieve these long-term rates and heat recovery, the heat exchange drainage volume (HEDV) of the reservoir must be considerably larger than those in previous EGS projects. The HEDV of the reservoir can be increased using horizontal wells with extended laterals by creating more induced fracture networks between horizontal wells with multistage fracturing techniques or accessing larger volumes of natural fractures or porosity systems.

To prevent the fluid from short circuiting between the injector and producing wells, flow and temperature needs to be detected, and modified to ensure that the heat is harvested from the entire volume of hot rock to maintain the rates and fluid temperatures needed for the electrical generation plant. Additional hot fluid can be added to the system with a natural heated system, such as a binary power plant used in co-generation electrical generation plants, to provide sufficient additional heat and overcome the normal decline in heated water production from an EGS project. Heat also can be added to the produced water by burning fossil fuels which will extend the areas of possible EGS development, and over come natural heat declines in the produced water over time. The combination of geothermal heat with other heat will lower the overall unit emissions for the power generated and increase the cost competiveness of the EGS system, particularly as experience is gained and natural cost and resource optimizations occur. This could accelerate the system adoption and speed the energy transition.

FORGE Wells

There are a variety of well penetractions at the FORGE site (Figure 2-C). A FORGE deep well indicated *a crystalline thermal reservoir (granitoid)* with temperatures exceeding 197 ºC at less than 3 km depth (Allis et al., 2016). Furthermore, the following are the existing or planned extended reach wells to demonstrate EGS technologies:

Well 16A (78)-32: FORGE Well 16A (78)-32, a deep inclined *water injection well* **(**65 º deviation with respect to the vertical in the deeper part of the well), was completed in January 2022 (England and McLennan, May 2022). Specifically, this well is vertical to a depth of about 6200 feet, deviates from vertical at 6200 feet until to 7200 feet where the well continues on a straight-line slanted course until it reaches a depth of 8540 feet. The measured depth (MD) at the toe of the well is 10938 feet.

During the period of April 14-24, 2022, three intervals in Well 16A(78)-32 were successfully

stimulated at depth greater than 10,000 feet MD. The first hydraulic fracture stage was completed open hole at the toe of the well followed by stages 2 and 3 hydraulic fractures in two shallower intervals of 20 feet within the casing.

Well 16B(78)-32: In late 2022 or early 2023, a second deep deviated well, FORGE Well 16B(78)-32, a *water production well*, will be drilled to intersect the three hydraulic fractures of Well 16A(78)-32.

Well 58−32: This well was drilled in 2017 as an observation well and to measure reservoir properties—rock type, temperature, permeability and stress in the reservoir.

Well 56-32 and Well 78B-32: Well 56-32 (MD 9145 feet), Well 78B-32 (MD 9500 feet), and Well 58-32 (MD 7536 feet) have been instrumented with fiber optics, discrete acoustic sensors (DAS) and geophones to gather and triangulate microseismic data to determine fracture geometry, etc.

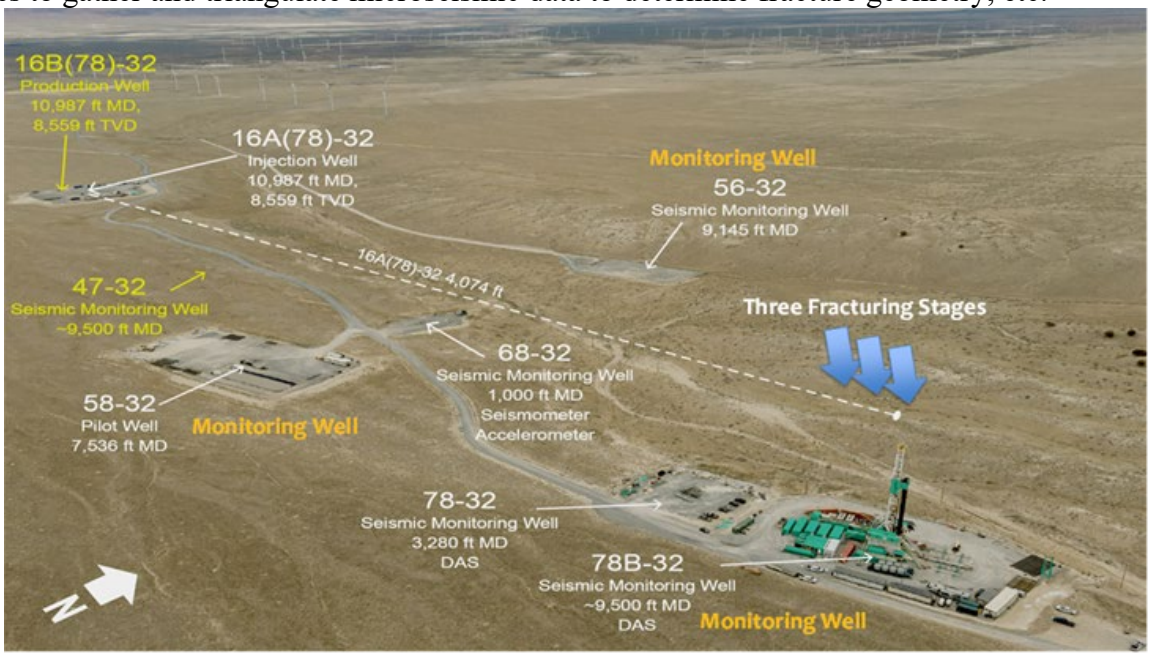

Figure 2-C: Aerial view of the wells drilled at the Utah FORGE site and the location of the three frac stages. (Source: UTAH FORGE, U.S. DOE)

Enhanced Geothermal Systems (EGS) History

Enhanced geothermal systems (EGS) evolved from the hot dry rock concept (HDR) project implemented by Los Alamos National Lab at Fenton Hill in 1977. The results demonstrated that heat could be extracted at reasonable rates from a hydraulically stimulated region of low-permeability hot crystalline rock. The history of EGS Systems is chronicled, with a thorough list of references, in the paper "Enhanced Geothermal Systems (EGS): A Review" (P. Olasolo, 2016). Unlike conventional geothermal reservoirs that are dominated by hydrothermal convective heat transport, the HDR concept is dominated by conduction only. The strategy of EGS has evolved to the creation of subsurface geothermal reservoirs in practically impermeable hot granitoid rock. This reservoir would be created by inducing hydraulic fractures and opening pre-existing natural fractures and fissures resulting in a subsurface heat exchanger. Water or other liquids with lower boiling points could be used as an injectant into the newly created system of subsurface fracture network, to extract the thermal energy from the surrounding rock. Hot water would be produced from the production well and used to generate electrical power at the surface power plant.

Multi-stage fracturing of horizontal wells for geothermal completions were described in several publications (Eustes et. al, 2018). A review of previous attempts to use shale development techniques in EGS can be found in "Review of Recent Unconventional Completion Innovations and their Applicability

to EGS Wells" (Gradl et al. 2018). More recently, a paper (Guinot and Meier, 2019) described the unsuccessful efforts to develop an EGS at the Basel Deep Heat Mining (DHM) project, and reviewed concerns over induced seismicity, as well as reviewed multi-stage stimulation in the oil and gas industry and its applicability to future EGS projects.

On February 24, 2021, DOE announced that the University of Utah had selected multiple projects to receive funding for EGS technology development and demonstration. Projects were chosen to develope devices suitable for sectional (zonal) isolation along both cased and open-hole wellbores under geothermal conditions and also for stimulation and configuration of the well (s) at Utah FORGE. One such EGS technology is described in the patent application US 2020/0217181A1 by Norbeck and Latimer (2020) who explained that many prior unsuccessful attempts in EGS was due to the inability to access enough heated rock with the injected water. Specifically, this shortcoming was caused by the injected water quickly breaking through, or short-circuiting between the injector and the producing wells, thus not harvesting much of the available heat. Norbeck and Latimer proposed a system to overcome the aforementioned difficulties in their patent application.

Multi-Stage Fracturing Tools Used in Oil and Gas Industry

Multi-stage fracturing of horizontal wells began approximately 30 years ago in the Barnett Shale in Texas. Prior to that technology development, fracture stimulation of an many horizontal wells were performed in one single stage using a variety of methods to attempt to divert the frac fluid throughout the entire well. Tools such as frac baffles were used with perforating to improve coverage in vertical and directional wells, but horizontal wells provided special difficulties due to the need to convey tools and guns into the horizontal section. Frac sleeves, which are mechanically simple with a port and an inner tubular that moves downward when a frac ball lands in a landing rig were effective in decreasing the time between stages and improving the well economics, which improved with more stages and longer laterals. Many frac sleeves have been successfully used in the oil and gas industry. The legacy and most existing frac sleeves rely on a series telescoping balls of increasing size to open sleeves, which had the drawback of smaller cross-sectional areas of the landing rings toward the distal part of the wellbore, and a limitation on the number of sleeves with corresponding sized ball that could be used.

"Plug and Perf" became the dominating shale well completion method, with perforating guns equipped with addressable switches and easy to drill composite bridge plugs, plus a variety of other innovations to cut costs and improve productivity. The primary limitations which complicate the use of "Plug and Perf" for EGS are the elevated temperatures which lead to high stresses and material/electronics failure which limit conventional stimulation efforts as seen in the packer used at FORGE well 58-32 (Figure 3) or the composite plugs temperature limitations and the need to be removed by drilling after the multistage fracturing process. Drilling plugs out in large diameter wellbores is difficult and expensive due to small diameter coiled tubing buckling as it supplied weight on bit (WOB) to drill out the plugs, leading to the lock up of the coiled tubing before the entire horizontal length of the lateral can be cleaned out. Further, the perforation tunnels that are created during "Perf and Plug" are in the well forever. These perforations complicate the need to control the injection fluid in wells to prevent "short circuiting" of fluid between injectors and producing wells, which must be controlled with diverters or packers and inner tubing strings.

Figure 3: Well 58-32 packer damage

Conventional stimulation tools have a variety of inherent limitations for EGS applications, but these are the most critical:

1. Packers and bridgeplugs have a variety of leak paths that must be sealed with elastomers in the presence of severe thermal stresses resulting from high geothermal temperature,

2. Packers and bridgeplugs must grippingly and sealingly engage the wellbore, and maintain the seal throughout the life of the EGS well in the face of geothermal temperatures,

3. Packers and tubing strings either increases the diameter of the wellbore to support desired injection and production rates or limits those rates,

A key goal of FORGE is to overcome these problems that current technology limitations make EGS systems too expensive and inefficient. to avoid packer failures such as those documented in the photo above and the report “FORGE 58-32 Injection and Packer Performance – April 2019”.

GeoThermOPTIMAL EGS System

Another of the FORGE proposals receiving funding developes devices suitable for sectional (zonal) isolation is called GeoThermOPTIMAL. This project improves upon the existing EGS technologies by the development and use of next generation multi-purpose sleeves, called FracOPTIMAL sleeves, that are made up with and run into a horizontal wellbore and cemented in place. This sleeve uses a new casing frac sleeve design, which would be cemented in the wellbore and uses a ball to shift a sleeve for multi-stage stimulation operations. Cemented frac sleeves have been successfully used in oil field operations

since at least 2006 (Rytlewski, 2006). Cemented sleeves have also proven that cement sleeves can successfully initiate fractures through cement without perforations (Bozeman, 2009). (Stegent, 2011), Cemented casing sleeves minimize the large thermal effect forces acting on the downhole equipment due to temperature changes in the unrestrained tubulars between packers. The casing sleeves can be used with packers, but in the preferred method, are cemented in the wellbore, with the cement hardening to provide annular isolation between the sleeves, and to distribute forces from the casing to be resisted by the encapsulating cement, lowering the resultant stresses in the tubulars and sleeves,

Technology development also evolved to permit the use a dissolvable ball for zonal isolation, removing one of the major barriers to the use of frac sleeves. The balls dissolution clears the wellbore for EGS operations with no further wellbore interventions. The preferred balls will be single sized, near casing drift diameter, with the flexibility for use in all casing or wellbore sizes. After the cement hardens and the drilling rig is released, these sleeves are first used for multi-stage fracturing, using the cement to encapsulate the sleeves and the casing to provide both annular hydraulic isolation and distribution of the extreme thermal axial stresses associated with geothermal wells to the cement sheath. A preferred application would use the intersection of induced fractures from each of the stages from the injection wells with one or more open hole or "barefoot" producers. These fracture intersections with the open hole section of the producers would be detected by surface pressure measurements in the producers. This is similar to the use of Sealed Wellbore Pressure Monitoring (SWPM) in shale development wells (Haustveit et al, 2020), with the key difference that when the fracture intersects the producer the pressure response would be much more obvious, and the fluid could flow to the surface through the producing wells. The flow from the injector to the producer could continue through the induced fracture, even after the fracture stage is complete, draining the stimulation fluid, and pressure that would be trapped in the previous stage(s), reducing the horizontal stress in the rock, The pressure relief of the previous stages would reduce significantly the needed treating pressures on subsequent stimulation stages and would allow the rapid recycling of the fracturing fluid "trapped" in the previous stage through the producing wellbore back to the stimulation fluid system for use in subsequent stimualtion stages. This would also significantly lower the water requirments of the total stimulation, and reduce the formation stresses, which could significantly reduce the induced seismicity associated with the stimulation operations.

After the multi-stage fracturing treatments, the dissolvable balls would leave the wells be ready for immediate injection operations. All subsequent operations for conformance control of the EGS would occur inside the cooler injection wells, which are cooled by the large volumes of injection water from the surface. This system is depicted in Figures 4 and 5, creating a subsurface heat exchanger for EGS application. This heat exchanger consists of a series of multistage hydraulic fractured horizontal wells, with blue injectors and red producers.

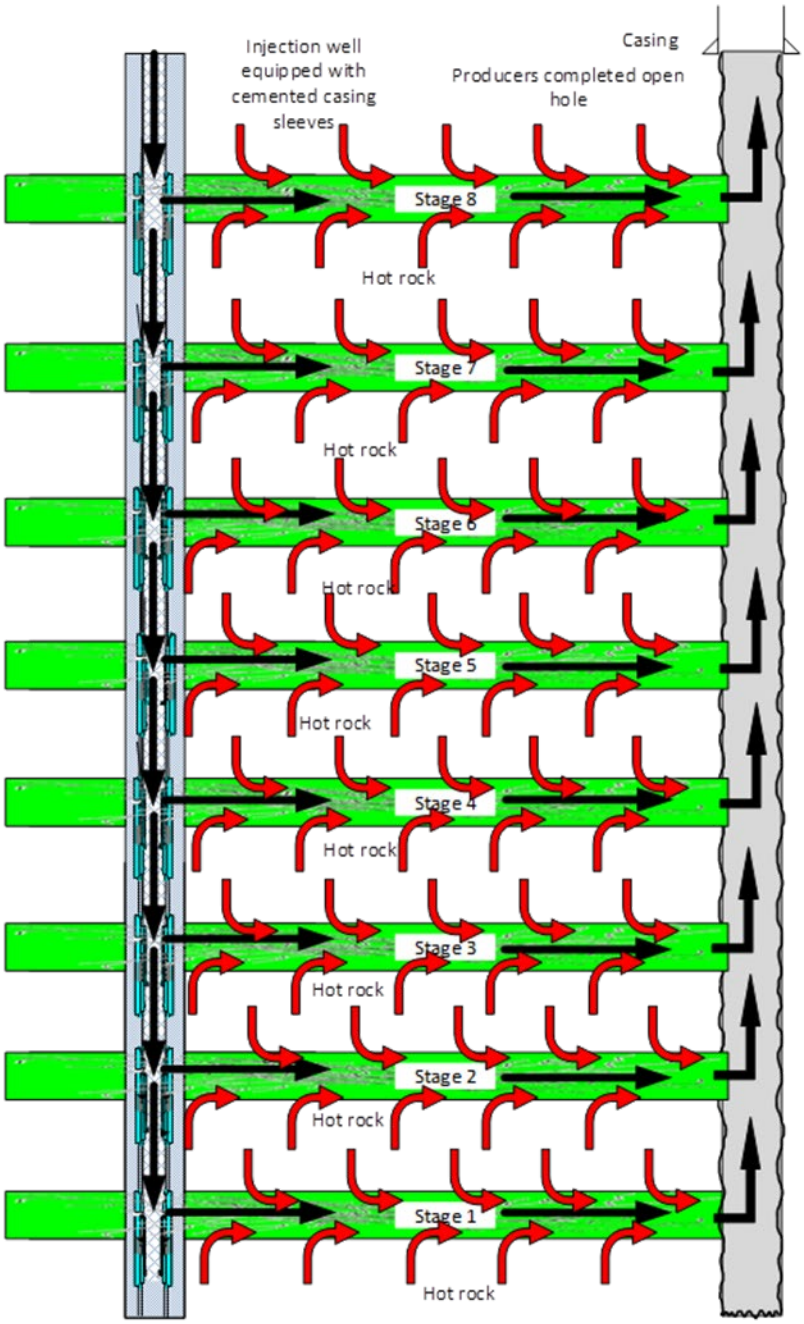

Figure 4: GeoThermOPTIMAL EGS System, Ideal Operating Conditions

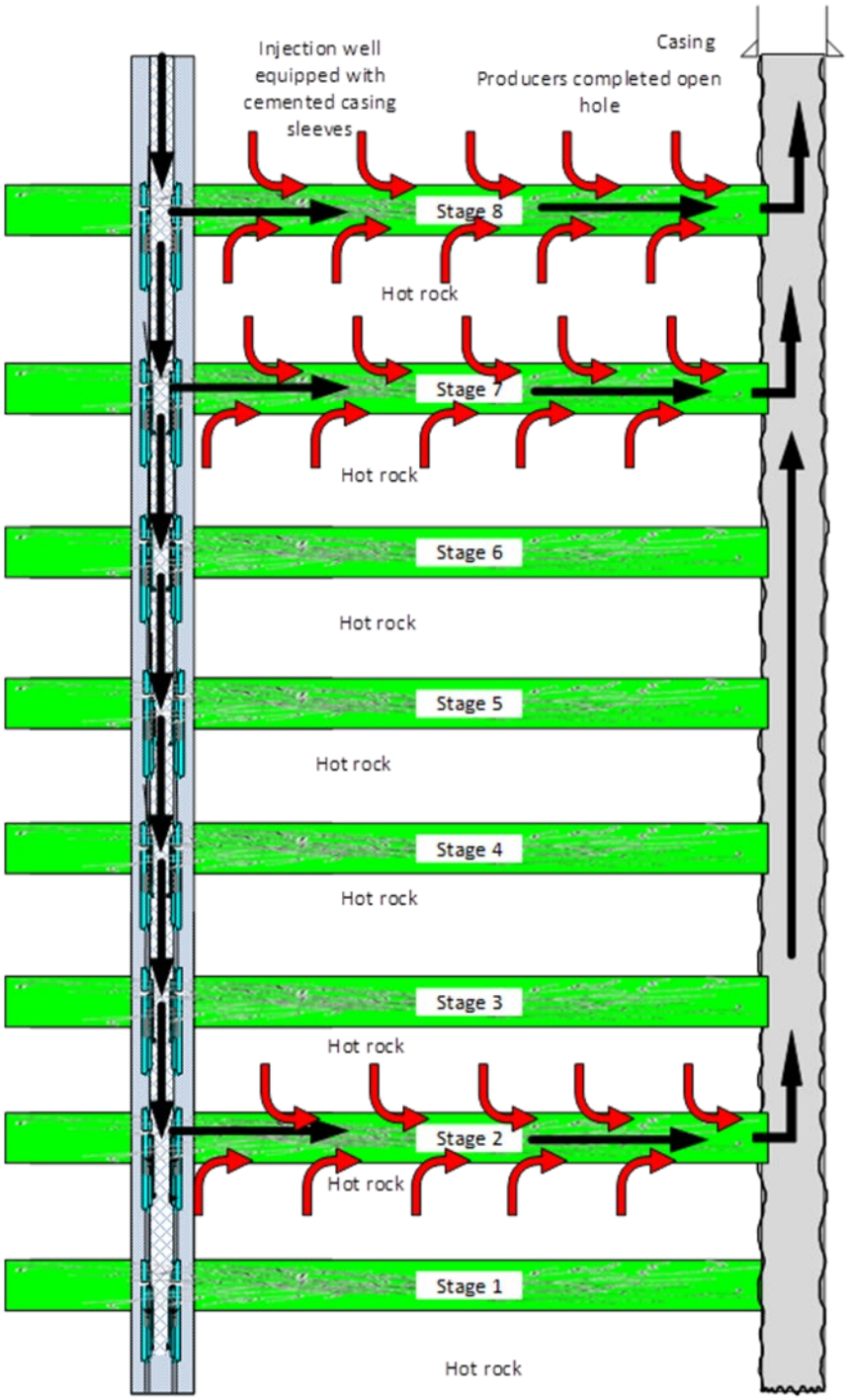

Figure 5: GeoThermOPTIMAL EGS System, Fluid "Short Circuiting"

Cemented Frac Sleeve

The frac sleeve under development is a unique sliding sleeve conceived by Colorado School of Mines and developed by Tejas Research & Engineering in response to technology gap in subterranean geothermal well technology, where a hot subterranean formation (hot rock) is used as a heat exchanger. The sleeve has two essential functions:

1. Flow control – to enable the operator to prohibit or divert ambient water to selected regions of the well to enable production of the hottest possible steam.

2. Multi-stage stimulation – to enable a single diameter ball to be utilized during multi-stage fracturing in each sleeve location to enhance formation permeability and porosity.

In EGS operations, a cold-water injection well delivers water to the formation for harvesting heat, the water passes through fissures and cracks to a second well where steam or hot water is produced, with a primary objective of spinning a turbine and generating electricity. The well-known problem in geothermal wells is the degradation of steam temperature due, in part, short circuiting of water between wells. The solution sought is to enable the selective diversion of ambient water into different locations of the subterranean formation by opening and/or closing a linear array of sliding sleeves in the well.

For instance: Where three sleeves are deployed in a geothermal well, S1, S2 and S3, if S1 is open and S2 and S3 are closed. When temperature degradation is detected, S1 can be closed and either S2 and S3 and be opened by means of a tractor that has keys to engage a recess in a shiftable sleeve section of the tool. Use of the sleeve and the tractor enable selective opening and closing of sleeves in the long term without reliance on an sensors and actuators (either electric or hydraulic) embedded in the sleeve that are likely to fail prematurely in the high temperature environment. Use of a surface deployed high temperature tractor, specially adapted to this task, assures that an actuating means is always available when needed.

Another important advantage of use of this sleeve is during well construction where sttimulating the formation is required to enhance porosity and permeability. The unique **Flow Rate Opening Logic** (see detailed explanation hereinafter) and deployment of a well-known dissolvable frac ball comprises very novel and useful features when initially stimulating the well. When a frac ball is pumped at a high Rate, the ball passes through the sleeve landing collets using high pressure and rates controlled at the surface pumps to traverse that sleeve, with a pressure spike to record the passage, to a sleeve below. When the frac ball is pumped at a low rate and pressure, the ball stays lodged in the landing collet and the hydraulic metering system in the sleeve releases the Inner Sleeve for shifting downwards thereby opening ports on the sleeve. Now the desired section of the formation shall be stimulated. The multi-stage stimulation procedure shall typically begin in the most distal sleeve sleeve toward the toe of the well and stimulation proceeds sequentially from the toe to the heel of the lateral. The process is repeated until every sleeve has been opened, and the adjacent formation is stimulaed. Each sleeve is open as the balls dissolve, but then can be closed (or re-opened) with a tractor.

Sleeve Design Parameters

Three sleeves shall be deployed in the FORGE test wells previously described on 7” casing in a 9.500” open-hole and cemented in place. Shut-in bottom hole temperature is specified at 225 °C (437 °F), and the tools will be tested in fixtures, first at ambient and the service temperatures to confirm the sleeve capabilities. The outside diameter of the sleeve is 8-3/4”, leaving a radial clearance of 3/8” per side. This compares to standard field proven frac sleeves which also has 3/8” clearance per side, or 3/4" diametrically.

The tractor shall pass through all the sleeves so there are two critical internal diameters to consider. The first are the sleeve End Housings at 5.950” – a diameter which is .030 larger than the diameter of the casing. The internal shiftable sleeves have an inside diameter of 6.080” which is approximately .132” larger than the inside diameter of the End Housings. This difference in diameters is essential to enable the unique opening logic symbiosis between the shiftable sleeves, the frac ball and the differential fluid rates. Moreover, the flow area of the ports is 38 in^2 which is approximately 37% larger than the flow area of the casing at 27 in^2. Significantly, because the port area is larger than the casing area, the injection fluid velocity will always be greater in the casing than the ports, assuring longevity regarding erosion. The sleeve landing collets is adapted for a “dissolvable” frac ball size of 5.75”.

The final essential design parameter is that the shiftable sleeves shall have a profile to enable keys on the tractor to engage. The tractor’s function, once engaged, is to shift the open sleeve, to the closed position.

Unique Flow Rate Opening Logic

1. High Rate – Ball Trips Thru (Inner Sleeve cannot respond quickly, fluid metered response)
2. Low Rate – Metering system releases the Inner Sleeve for shifting (similar to a hydraulic jar – loses its fluid resistance at a particular stroke)
3. Re-closeable with a tractor, in an Upper Inner Sleeve Profile
4. Transitable by tractor – easy to roll through
5. Inside diameter of the sleeve is larger than the drift ID of the casing
6. Rapid, Hi-Flow Rate Ball passed through the Lower Tripping Collet – Damping in Play
7. A slower Flow Rate Ball allows the Hydraulic Damping System and Power Spring to "Deactivate" allowing the Inner Sleeve to fully OPEN for stimulation operations
8. The upper Shifting Profile is used to Pull the Sleeve CLOSED. Once almost closed, the Power Spring re-activates helping assist with closing the Sleeve
9. Low Cement fouling areas – Simple, proven functionality

Figure 6: Isometric Model of FracOPTIMAL Sleeve

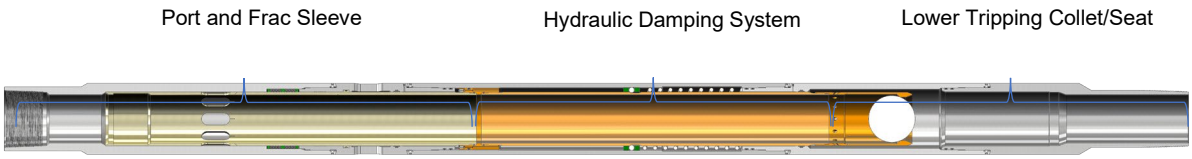

Figure 7: Cross Section of Prototype Sleeve Concept

Well Completion Data

Open Hole Diameter: 9.500"
Casing size; 7"
BHT 225 °C (437 °F).
OD – 8.750"

Minimum ID – 5.940”
Radial Clearance = 0.375”
Standard Frac Sleeve = 0.375”
ID – 5.950” +.010/-.000 (End Housings, 0.030” Over ID)
ID – 6.080” +.010/-.000 (Internal Sleeves)
ID Flow Area – 27.802 inches.
Ported Flow Area – 38.18 in2 (1.37X Factor)
OAL – 146” (just over 12’)
Frac Ball Size – 5.75”

High Temperature Tractor

The high temperature tractor assembly design utilizes proven oil and gas high temperature operational technologies. The base components of the assembly will consist of a monocable high temperature wireline, a high temperature cable head, a high temperature swivel joint, a high temperature CCL for depth control, a sensor sub that will provide high resolution temperature and pressure real time, an electromechanical wheeled tractor, and a hydraulic driven actuator for sleeve control.

From the cable head to the sensor sub all the technologies used in this design are currently being operated in oil and gas operations up to 500 ^{o}F. These technologies date back to development in the early 90s. The tractor portion of this system will consist of a flask electronics section and the tractor drive section. The electronics section will consist of multiple PC boards rated and tested to 175 ^{o}C/350 ^{o}F continuous operation. These electronics will be housed in an integral Dewar flask with low thermal leakage and internal heat sink to allow the electronics to operate below rated temperature of 225 ^{o}C for a duty cycle of 12 hours. This duty cycle should allow for adequate time to locate each of the three sleeves to close or open as needed. The tractor assembly drive components will be modeled on current tractor hardware in the oil and gas industry. The drive assembly will consist of drive wheels that make contact with the casing wall to move the assembly up and down the borehole. Once the tractor assembly has moved the full string into the location of the sleeve, the sleeve latch assembly which consist of an anchor mechanism and hydraulic piston/latch mechanism will be actuated. The latch locating will be done using pressure monitoring of the latch assembly pump to come in contact with the sleeve. Once located in the proper contact position of the sleeve, the open and close function can be performed. This cycle of operation can be performed repeatedly within the duty cycle of the temperature rating of the flask electronics. Following downhole operations, the tractor will be retrieved to the surface by the wireline unit.

Modeling

In addition to describing the tool innovation for creating the EGS, the paper presents *mathematical modeling* in support of (1) tool design and its implementation to assess the success of reservoir stimulation in the FORGE geothermal reservoir site in Utah, and (2) evaluating well stimulation efficacy, effective stimulated formation permeability, and formation storativity via diagnostic fracture injection test (DFIT) and tracer injection-backflow test in the same well. The reservoir characterization components of these mathematical models will be similar to what have been developed in the past two decades and used in assessing unconventional reservoirs. The mathematical modeling includes several components and activities:

(a) Develop a wellbore heat transfer model to determine the temperature profile for cooling during the use of the well stimulation device, and to determine the needed duty cycle during tractor and non-tractor electronics based on temperature thresholds of components under a variety of pumping and temperature scenarios.

(b) Develop a reservoir heat exchange model to determine the efficacy of heat extraction from the reservoir hot formation rock and reservoir fluid to deliver the heated water in the

wellbore heat exchanger to the power plant. ***The presence or absence of hot water in permeable geothermal site is very critical to the success of heat recovery!***

(c) Assess viability of the discrete fracture network (DFN) and its value in quantifying formation stimulation and heat extraction from the formation

(d) Evaluate past tracer concentration response and DFIT pressure response from field and conceptual model data to recommend future tests to quantify the efficacy of the fracture network resulting from well stimulation

(e) Assess rock deformation resulting from temperature change during well stimulation and future operation of the EGS

The details of the above plan are:

(a) The wellbore heat transfer mathematical modeling. The associated physical mode is a downhole coaxial heat exchanger where the working fluid is contained within the wellbore and without any seepage into the surrounding rock formations (Figures 3-A, 3-B, and 3-C). We will use Eq. 1 in the immediate vicinity of the injection well and Eq. 2 further away from the wellbore:

$$-\rho_w C_w \left(u_{w,z}\right)\frac{\partial T}{\partial z}+\left[\frac{1}{r}\frac{\partial}{\partial r}\left(rK\frac{\partial T}{\partial r}\right)\right]_{r_1}=\rho_w C_w \frac{\partial T}{\partial t} \tag{1}$$

$$\frac{\partial}{\partial x}K_x\frac{\partial T}{\partial x}+\frac{\partial}{\partial y}K_y\frac{\partial T}{\partial y}+\frac{\partial}{\partial z}K_z\frac{\partial T}{\partial z}=\rho_s C_s\frac{\partial T}{\partial t} \tag{2}$$

If the surrounding rock formations are permeable and contain flowing hot water, we will include the following equation, Eq. 3, to our model to continue reheating the wellbore rock region with heat from the flowing water.

$$\nabla\cdot\left[\frac{k}{\mu}\left(\nabla p_w-\gamma_w\nabla D\right)\right]=\frac{1}{M}\frac{\partial p_w}{\partial t}-\phi\,\alpha_{T,w}\frac{\partial T_w}{\partial t}-\alpha\frac{\partial \varepsilon_v}{\partial t} \tag{3}$$

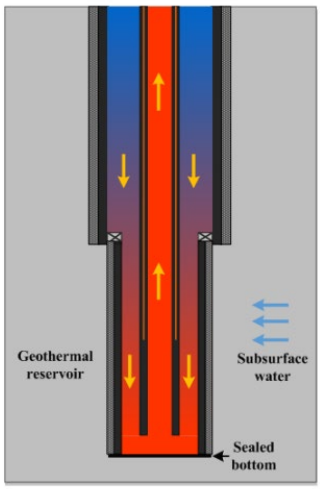

Figure 8-A: Downhole coaxial heat exchanger in single-well geothermal heat extraction (from: Zheng et al.: Heat extraction performance of a downhole coaxial heat exchanger geothermal system by considering fluid flow and temperature gradient in FORGE Well 58-32, GRC Transactions, Vol. 42, 2018.

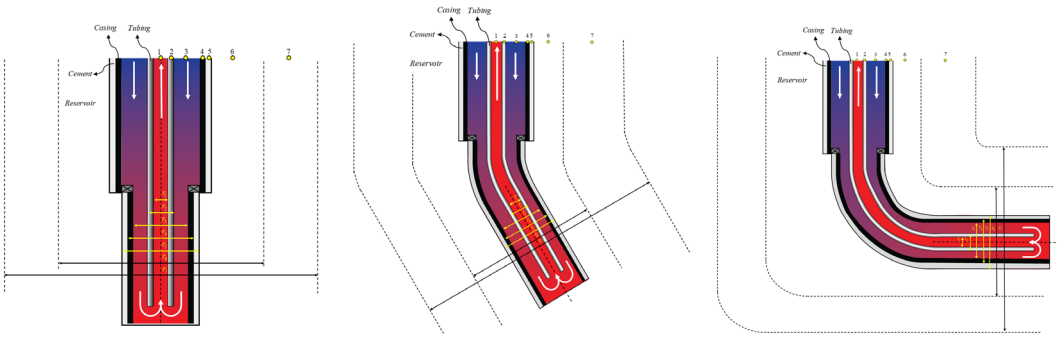

Figure 8-B: Three potential coaxial heat exchanger in single-well geothermal heat extraction.

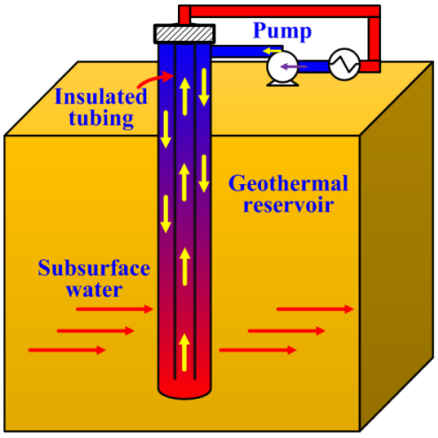

Figure 8-C: Single well downhole heat exchanger model (Zheng et al. 2018)

We will also use the following geothermal wellbore heat exchange model (Figure 9) for assessing coil tubing heating-and-cooling by injecting cold water into the coil tubing. Contrary to the earlier single-well, downhole heat exchange model, there is no casing downhole; thus, there will be fluid seepage into the formation during cold water circulation. To accommodate this configuration, we need to flow model that includes wellbore pressure calculation. The equation that will be used is Eq. 4.

$$\nabla\cdot\left[\frac{k}{\mu}\left(\nabla p_w-\gamma_w\nabla D\right)\right]+\hat{q}=\frac{1}{M}\frac{\partial p_w}{\partial t}-\phi\,\alpha_{T,w}\frac{\partial T_w}{\partial t}-\alpha\frac{\partial \varepsilon_v}{\partial t} \tag{4}$$

Where,

$$\hat{q}=q_w/\left(2\pi r_{well}\Delta r\Delta z\right)$$

$$q_w=-WI(p_{w,formation}-p_{w,well})$$

$$WI=2\pi\frac{k}{B\mu}\frac{\Delta z}{\left[\ln\left(\frac{r_b}{r_w}\right)+s\right]}$$

$$p_{w,well}=\left(p_{w,surface}+\gamma_w Depth\right)+h_f$$

$$h_f=f\left(\frac{Depth}{d_{tubing}}\frac{v_{w,tubing}^2}{2g}\right)$$

$$f=64/N_{\mathrm{Re}}\ \text{for}\ N_{\mathrm{Re}}<2000$$

$$\frac{1}{\sqrt{f}} = 1.74 - 2\log\left[2(\varepsilon/d) + 18.7/(N_{\mathrm{Re}}\sqrt{f}\right] \quad \text{for } N_{\mathrm{Re}} > 4000$$

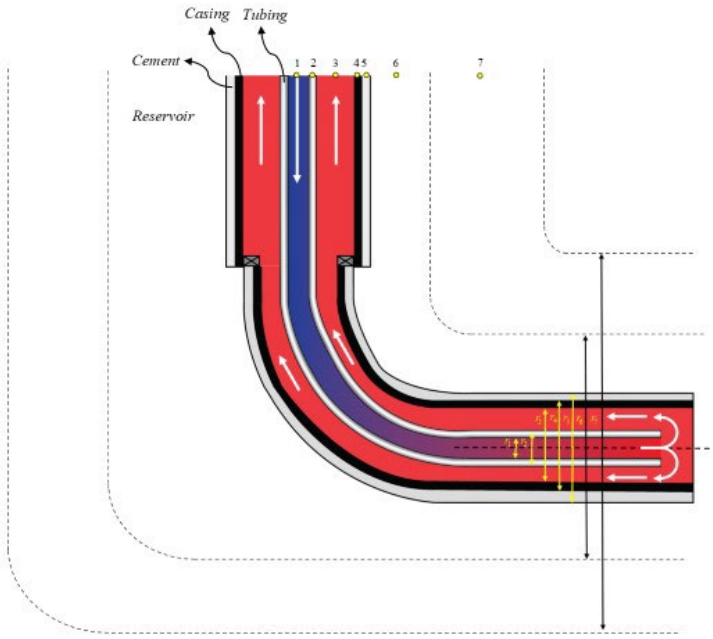

Figure 9-A: Geothermal reservoir heat exchange model (with casing in the entire well) for evaluating working fluid heating and cooling in GeoThermOPTIMAL tool design.

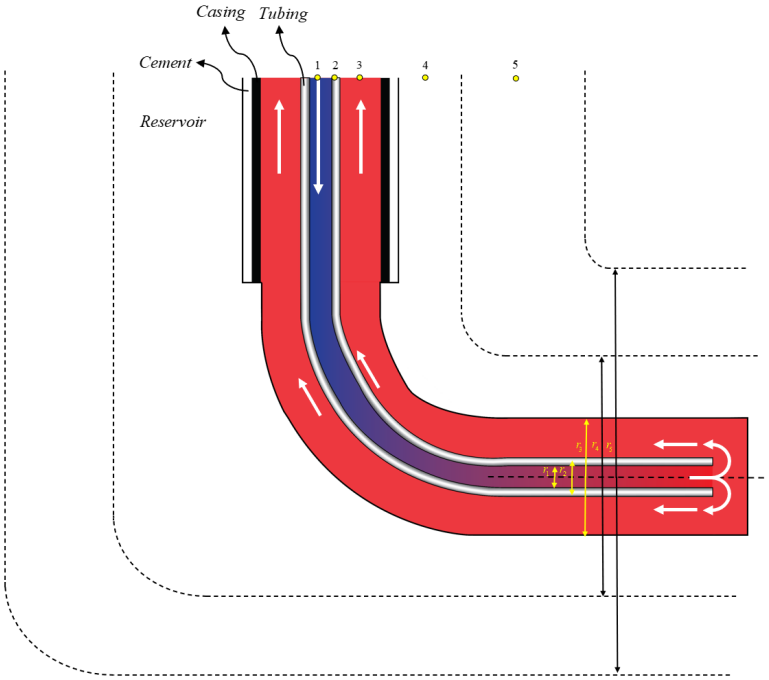

Figure 9-B: Geothermal reservoir heat exchange model (with open hole completion in the horizontal section) for evaluating working fluid heating and cooling in GeoThermOPTIMAL tool design.

(b) The reservoir heat exchange model, Figure 10, includes heat advection in the hydraulic fractures and heat conduction at the fracture-rock interface, that is:

Without leakoff

$$\underbrace{-\left(\rho_w C_w u_{w,f}\frac{\partial T_f}{\partial x}\right)}_{\text{Heat Advection in HF}}\underbrace{-\left[-\left(\frac{K_y}{w_f/2}\right)\frac{\partial T_m}{\partial y}\bigg|_{y=w_f/2}\right]}_{\text{Conduction of Heat at the Fracture-Matrix Interface}}=\underbrace{\rho_w C_w\frac{\partial T_f}{\partial t}}_{\text{Rate of Heat Accumulatio in the Fracture}} \tag{5-A}$$

With leakoff

$$\underbrace{-\left[\rho_w C_w\left(\frac{\partial}{\partial x}\left(u_{x,w,f}T_f\right)\right)\right]}_{\text{Heat Advection in HF}}\underbrace{-\left[-\left(\frac{K_y}{w_f/2}\right)\frac{\partial T_m}{\partial y}+\rho_w C_w\frac{\partial}{\partial y}\left(u_{y,w,m}T_m\right)\right]_{y=w_f/2}}_{\text{Conduction and Convection of Heat at the Fracture-Matrix Interface}}=\underbrace{\rho_w C_w\frac{\partial T_f}{\partial t}}_{\text{Rate of Heat Accumulatio in the Fracture}} \tag{5-B}$$

$$\underbrace{\frac{\partial}{\partial x}K_x\frac{\partial T}{\partial x}+\frac{\partial}{\partial y}K_y\frac{\partial T}{\partial y}+\frac{\partial}{\partial z}K_z\frac{\partial T}{\partial z}}_{\text{Heat Conduction in the rock Matrix}}=\underbrace{\rho_s C_s\frac{\partial T}{\partial t}}_{\text{Rate of Heat Accumulation in the rock Matrix}} \tag{6}$$

Where,

$$u_{x,w,f}\big|_{x=0}=q_{inj}/\left(2w_f h\right) \tag{7-A}$$

In Eq. 5, the advection velocity $u_{x,w,f}(x)$ becomes smaller than $u_{x,w,f}\big|_{x=0}$ as water leaks off perpendicular to the hydraulic fracture face to the surrounding rocks. To account for the leakoff, we will use two approaches—one is a velocity leakoff model used in hydraulic fracture modeling and the second approach is to use Darcy velocity across fracture-matrix interfaac. The leakoff equation is:

$$u_{y,w,m}(t)\big|_{y=w_f/2}=C_L/\sqrt{t} \tag{7-B}$$

Where, $C_L=\left(\frac{k\phi\Delta p}{\mu}\right)^{1/2}$ for water displacing gas, $C_L=\frac{k}{\mu}\frac{\Delta p}{\sqrt{\pi\eta}}$ for water displacing water, and

$\Delta p=p_{w,f}(t)\big|_{y=\pm w_f/2,\ t>0}-p_R$

As another method to calculate advective flow components in x-y hydraulic fracture domain, we will use numerical solution of the following continuity equation. This equation will be constrained by Eq. 7-A and Eq. 7-B.

$$-\left(\frac{\partial u_{x,w}}{\partial x}+\frac{\partial u_{y,w}}{\partial y}\right)=c_t\frac{\partial p_w}{\partial t} \tag{7-C}$$

To solve Eq. 7-C for the velocity components in the fracture, we replace such velocities with the

Darcy equation which results in the following equation:

$$\begin{cases} \dfrac{\partial}{\partial x}\left(\dfrac{k_f}{\mu_w}\dfrac{\partial p_{w,f}}{\partial x}\right)_f + \dfrac{1}{w_f/2}\left(\dfrac{k_{f/m}}{\mu_w}\dfrac{\partial p_{w,f}}{\partial y}\bigg|_{y=w_f/2}\right)_f = \left(c_f + c_w\right)_f \dfrac{\partial p_{w,f}}{\partial t} \quad \text{(In half of HF)} \\ \dfrac{\partial}{\partial x}\left(\dfrac{k_m}{\mu_w}\dfrac{\partial p_{w,m}}{\partial x}\right)_m + \dfrac{\partial}{\partial y}\left(\dfrac{k_m}{\mu_w}\dfrac{\partial p_{w,m}}{\partial y}\right)_m = \left(c_f + c_w\right)_m \phi_m \dfrac{\partial p_{w,m}}{\partial t} \quad \text{(In 1/2 matrix next to HF)} \end{cases} \tag{7-D}$$

We solve Eq. 5A, Eq. 5B, and Eq. 6 numerically for the temperature, and similarly we solve Eq. 7-D for water pressure in the fracture and matrix using either an appropriate finite-difference or a mixed finite-element method. After obtaining the discrete pressure solutions, we will determine water velocity in the fracture and the leakoff using Darcy equation for the eventual use in Eq. 5-A and 5-B.

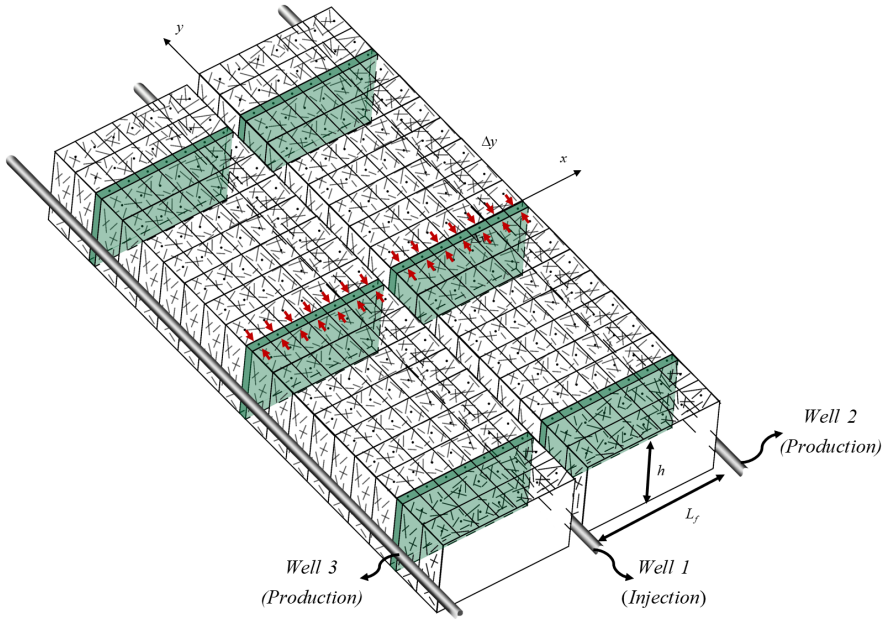

Figure 10: EGS consisting of one injector and two producers for extracting heat to generate electricity. The current casing sleeve prototype has an OD of 8.75 inches for use in a 9.5-inch hole at 225° C. The sleeve ID is 5.95 (end housing) and 6.08 (internal) inches.

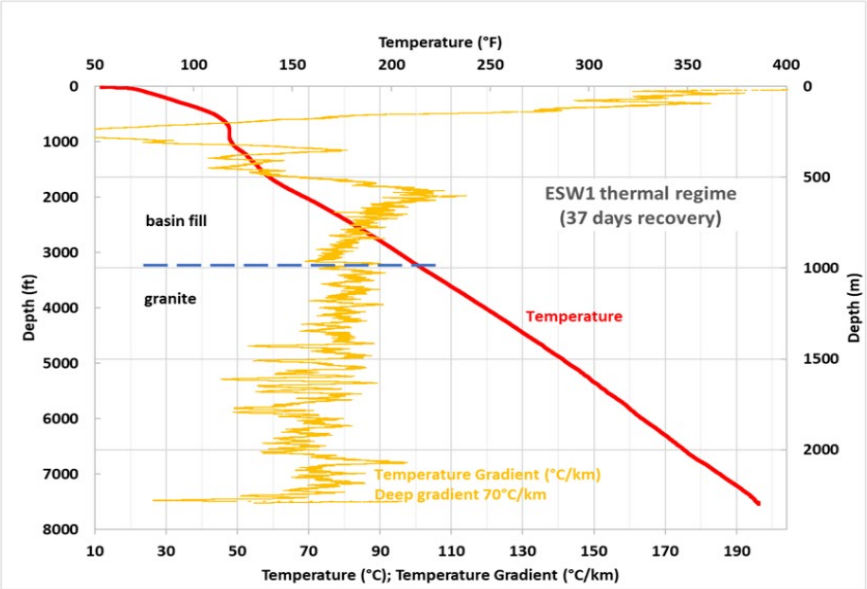

Figure 11: Thermal profile in Well 58-32, 32 days after drilling and testing (from: **Alice er al.**, GRC Transactions, Vol. 42, 2018).

(c) In assessing the effectiveness of DFIT (Figure 12 and DFN (Figure 13) flow modeling compared to advanced dual-porosity modeling techniques, we will compare the outcome of flow simulations using both model approaches on a well-defined fractured rock system. It is noteworthy that Nadimi et al. 2020 used *matrix permeability* of 2.9 E-17 m^2 (0.029 mD), *natural fracture permeability* of 1.0 E-15 m^2 (1 mD), and *hydraulic fracture permeability* of 5.0 E-11 m^2 (50,000 mD in their modeling effort. However, Nadimi et al. reported measured matrix permeability of 0.005 mD compared to 0.029 mD used in the modeling. We speculate that the 0.029 mD used in modeling represents effective rock permeability which includes micro- and macro-fractures resulting from hydraulic fracture stimulation. It is also interesting that the pressure falloff data of Figure 6 can be interpreted using the following pressure falloff analysis equation:

$$p\left(t_{inj}+\Delta t\right)\Big|_{x=0}-p\left(\Delta t\right)\Big|_{x=0}=\frac{4.064\,qB\mu}{\sqrt{k_{f,eff}}\left(h\;L_f\right)}\left(\frac{1}{\left(\phi c_t\right)_{f+m}\,\mu}\right)^{1/2}\left(\sqrt{t_{inj}+\Delta t}-\sqrt{\Delta t}\right) \tag{8}$$

To make use of Eq. 8, one should plot $p\left(t_{inj}+\Delta t\right)\Big|_{x=0}-p\left(\Delta t\right)\Big|_{x=0}$ vs. $\sqrt{t_{inj}+\Delta t}-\sqrt{\Delta t}$; then, identify a dominant straight line segment, and calculate the slope designated m which is related to reservoir properties: $m=\frac{4.064\,qB\mu}{\sqrt{k_{f,eff}}\left(h\;L_f\right)}\left(\frac{1}{\left(\phi c_t\right)_{f+m}\,\mu}\right)^{1/2}$ Knowing the slope m, one can calculate formation effective permeability $k_{f,eff}$. For practical reasons, if injection time is much larger than the shut-in time, we can plot $p\left(\Delta t=0\right)\Big|_{x=0}-p\left(\Delta t\right)\Big|_{x=0}$ vs. $\sqrt{t_{inj}+\Delta t}-\sqrt{\Delta t}$ and use the same slope equation given above.

Figure 12A presents data from injection-shut in tests conducted in FORGE Well 58-32 in 2017 and 2019. We have successfully applied the above analysis technique to Cycle 5 of injection-shut in tests conducted in FORGE Well 58-32 in 2017 (Figure 12B).

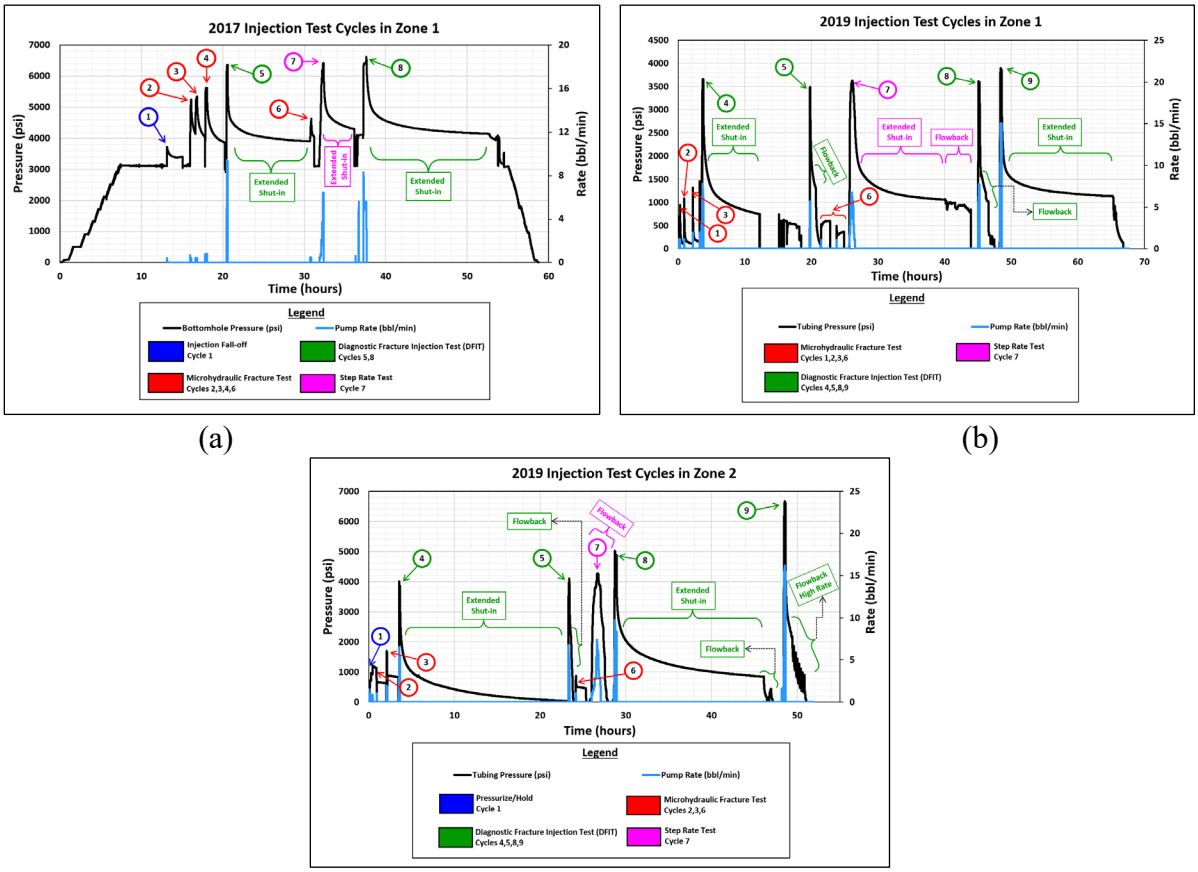

Figure 12-A: Injection and shut-in tests in FORGE Well 58-32: (a) Zone 1 in 2017 (b) Zone 1 in 2019 (c) Zone 2 in 2019 (From: Xing et al. 2020)

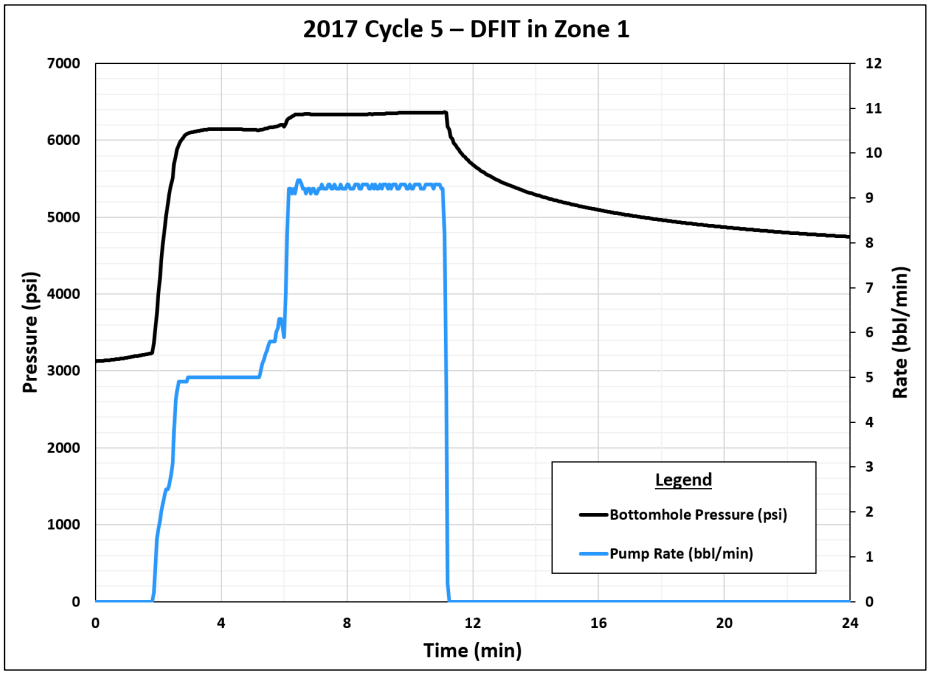

Figure 12-B: Diagnostic fracture injection test (DFIT) and stimulation borehole data

(reproduced from: Nadimi et al. Elsevier Geothermics 87, 2020)

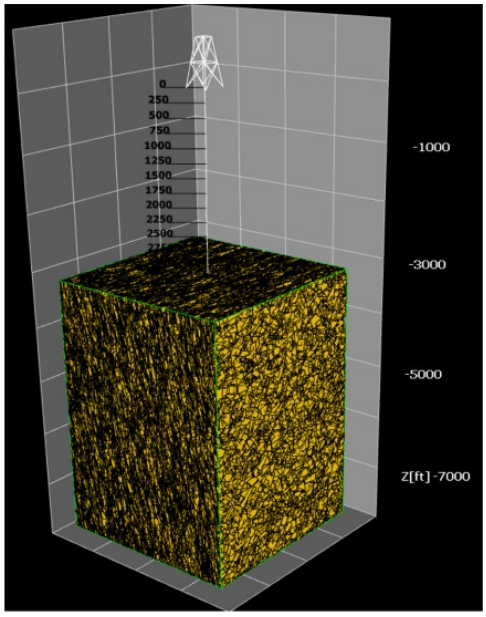

Figure 13: Best fit DFN model based on FMI fractures intersecting the Well 58-32 (Nadimi et al. 2020)

(d) To evaluate the use and effectiveness of tracers in characterizing the stimulated volume, we will analyze the past tracer concentration response from field and will generate conceptual model data for recommending future tests to quantify the efficacy of the fracture network resulting from well stimulation. The governing tracer transport equations are:

Fracture Medium:

$$D_{f,eff}\frac{\partial^2 c_f}{\partial x^2}-v_f\frac{\partial c_f}{\partial x}-\tau_c=\phi_f\frac{\partial c_f}{\partial t} \tag{9}$$

Matrix Medium:

$$\tau_c=\phi_m\frac{\partial c_m}{\partial t} \tag{10}$$

Where,

$$v_f=-\frac{k_{f,eff}}{\mu}\frac{\partial p_f}{\partial x} \tag{11}$$

$$\tau_c=\sigma\left[D_{m,eff}(c_f-c_m)+(k_m/\mu)(p_f-p_m)c_{f/m}\right] \tag{12}$$

$$\tau=\sigma(k_m/\mu)(p_f-p_m) \tag{13}$$

$$D_{m,eff}=\frac{\phi_m}{\tau_m}D_m \tag{14}$$

$D_{f,eff}$ = Effective dispersion coefficient in the fracture medium

$D_{m,eff}$ = Effective dispersion coefficient in the matrix medium

$v_f =$ Advection Darcy velocity

$\tau =$ Fracture-matrix advection transfer function

$\tau_c =$ Fracture-matrix tracer diffusion and advection transfer function

$\tau_m =$ Matrix tortuosity

We will be using the solution of the above equations in analyzing the tracer data of April 2022 in FORGE Well 16A(78)-32 (Figure 15). The goal is to characterize the reservoir for porosity and permeability in the vicinity of the hydraulic fractures.

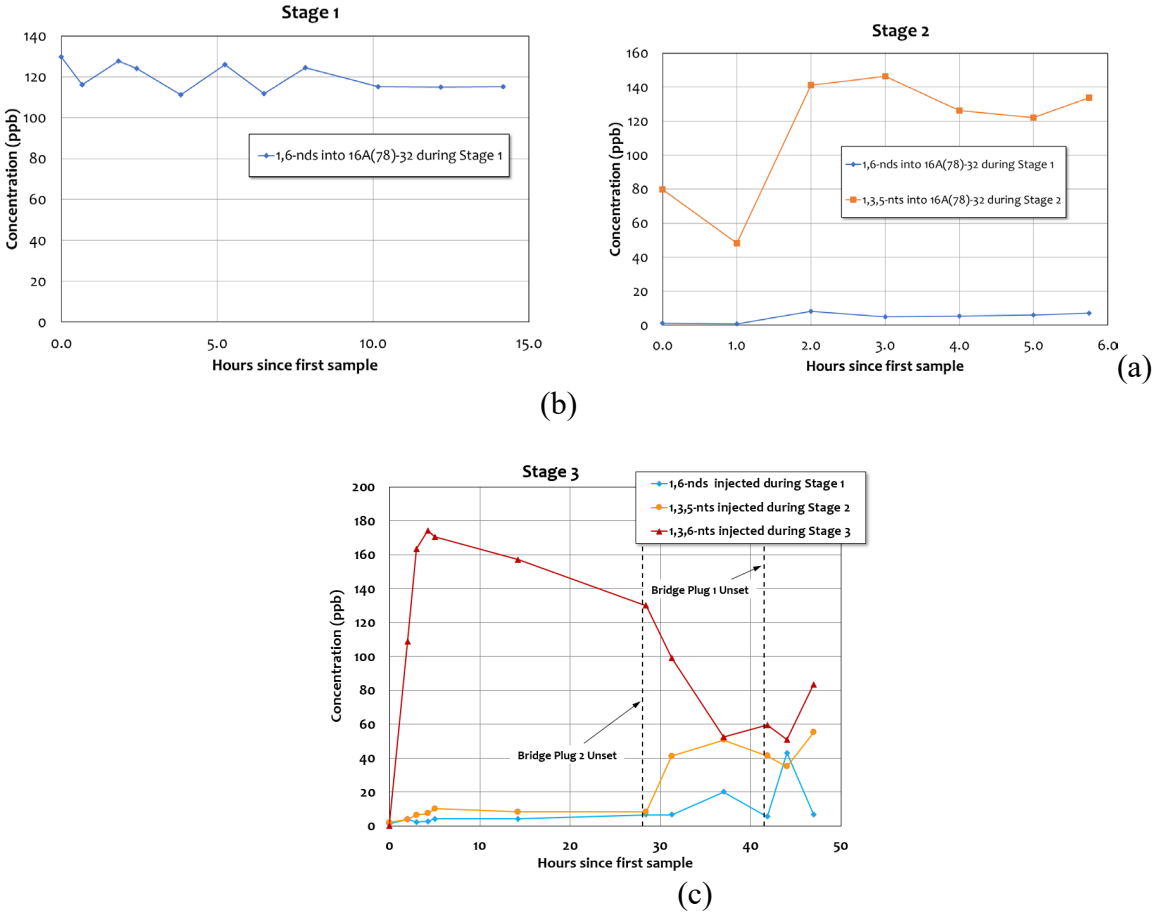

Figure 15: Tracer concentration response during the flowback in FORGE Well 16A(78)-32, April 2022. (a) Stage 1 (b) Stage 2 (c) Stage 3 (Source: Utah FORGE, U. S. DOE)

Auxiliary equations needed for use in tracer transport, etc. include a set of pressure equations and rock deformation equations given below (Uzun et al. 2017):

$$\nabla \cdot \left[\frac{k_{f,eff}}{\mu} \left(\nabla p_f - \gamma_{fl} \nabla D \right) \right] - \tau + \hat{q} = \frac{1}{M_f} \frac{\partial p_f}{\partial t} - \phi_f \alpha_{T,fl} \frac{\partial T_f}{\partial t} - \alpha_f \frac{\partial \varepsilon_v}{\partial t} \tag{15}$$

$$\tau = \frac{1}{M_m} \frac{\partial p_m}{\partial t} - \phi_m \alpha_{T,fl} \frac{\partial T_m}{\partial t} - \alpha_m \frac{\partial \varepsilon_v}{\partial t} \tag{16}$$

$$\tau = \sigma \left(k_m / \mu \right) \left(p_f - p_m \right) \tag{17}$$

$$\frac{1}{M_f} = \frac{\phi_f}{K_{fl}} + \frac{\left(\alpha_f - \phi_f\right)}{K_{dm}} \tag{18}$$

$$\alpha_f = 1 - \frac{K_{dfb}}{K_{dm}} \tag{20}$$

$$\frac{1}{M_m} = \frac{\phi_m}{K_{fl}} + \frac{\left(\alpha_m - \phi_m\right)}{K_{dm}} \tag{21}$$

$$\alpha_m = \frac{K_{dfb}}{K_{dm}} - \frac{K_{dfb}}{K_{sm}} \tag{22}$$

$$\alpha_m + \alpha_f = 1 - \frac{K_{dfb}}{K_{sm}} \tag{23}$$

$$G\nabla^2\vec{u} + (G+\lambda)\nabla\left(\nabla\cdot\vec{u}\right) + \vec{\gamma}_b = -\alpha_p\left(\nabla p - \gamma_{fl}\,\nabla D\right) - 3\alpha_{T,b}K_b\nabla T \tag{24}$$

Conclusion

The GeoThermOPTIMAL system improves the effectiveness of EGS well stimulation in such a way that it improves the efficiency of heat extraction for electricity generation by addressing two critical and long recognized problems specific to the construction and operation of a subsurface EGS heat exchanger:

1. The improved EGS system provides an effective multi-stage stimulation technology that has the speed of current shale development technologies but does not have the limitations of current stimulation tools and methods (such as the temperature limitations of conventional “Plug and Perf” stimulation technique or the need for coiled tubing cleanouts).

2. The EGS system leads to improved conformance control of the injected and produced water by minimizing ineffective water fingering between injection and production well pairs; thus, improving the heat recovery efficiency.

3. Finally, we believe that the use of dual well bores that are connected by the hydraulic fractures could reduce the increased formation stress from the earlier well stimulation stages by draining the water locked in the formation surrounding the earlier fracture stages. This could also reduce the risk of induced seismicity.

Nomenclature

$\alpha =$ Biot coefficient

$\alpha_f =$ Biot coefficient for fracture medium

$\alpha_m =$ Biot coefficient for matrix medium

$\alpha_{T,fl} =$ Fluid thermal expansion coefficient, $^{\circ}K^{-1}$

$\gamma =$ Fluid gradient, Pa/m

ε_v = Volume strain

η = Hydraulic diffusivity, m^2/s

κ = Thermal diffusivity, m^2/s

λ = Fluid mobility, 1/Pa . s

λ = Lame parameter, Pa

μ = Viscosity, Pa . s

ρ = Density, Kg/m^3

τ = Fracture-matrix pressure transfer function, s^{-1}

τ_c = Fracture-matrix tracer transfer function, s^{-1}

τ_m = Tortuosity of matrix pores

ϕ_f = Fracture porosity

ϕ_m = Matrix porosity

c = Fluid compressibility, Pa^{-1}

c_f = Tracer concentration in fracture medium, mole or weight fraction

c_m = Tracer concentration in matrix medium, mole or weight fraction

C_L = Seepage coefficient, $m/s^{1/2}$

D = Depth, m

$D_{f,eff}$ = Effective dispersion coefficient in the fracture, m^2/s

$D_{m,eff}$ = Effective dispersion coefficient in the matrix, m^2/s

G = Shear modulus, Pa

k = Permeability, m^2

k_f = Fracture permeability, m^2

$k_{f,eff}$ = Effective fracture permeability, m^2

$k_m =$ Matrix permeability, m^2

$K_{dfb} =$ Bulk ***drained*** modulus of matrix blocks containing fractures, Pa

$K_{dm} =$ Bulk ***drained*** modulus of ***matrix blocks*** without fractures, Pa

$K_{sm} =$ Bulk modulus of ***solid minerals*** in the porous medium, Pa

$K_{fl} =$ Bulk modulus of fluids in the pores, Pa

$L_f =$ Hydraulic fracture half length, m

$M_f =$ Biot modulus for fracture medium, Pa

$M_m =$ Biot modulus for matrix medium, Pa

$\lambda =$ Lame parameter, Pa

$p_f =$ Fracture pressure, Pa

$p_m =$ Matrix pressure, Pa

$r =$ Radial coordinate, m

$r_b =$ Well grid block radius, m

$r_w =$ Well radius, m

$s =$ Skin factor

$t =$ Time, s

$\tau =$ Fracture-matrix pressure transfer function, s^{-1}

$\tau_c =$ Fracture-matrix tracer transfer function, s^{-1}

$\tau_m =$ Tortuosity of matrix pores

$T_f =$ Fracture temperature, ^{o}K

$T_m =$ Matrix temperature, ^{o}K

$\vec{u} =$ Formation displacement vector, m

$\vec{u} =$ Formation interstitial velocity vector, m/s

$\vec{v} =$ Darcy velocity vector, m/s

$x, y, z =$ Cartesian coordinates, m

$w_f =$ Hydraulic fracture width, m

Acknowledgments

This material is based upon work supported by the Department of Energy, Office of Energy Efficiency and Renewable Energy (EERE), under Award Number DE-EE0007080. This report was prepared as an account of work sponsored by an agency of the United States Government. Neither the United States Government nor any agency thereof, nor any of their employees, makes any warranty, express or implied, or assumes any legal liability or responsibility for the accuracy, completeness, or usefulness of any information, apparatus, product, or process disclosed, or represents that its use would not infringe privately owned rights. Reference herein to any specific commercial product, process, or service by trade name, trademark, manufacturer, or otherwise does not necessarily constitute or imply its endorsement, recommendation, or favoring by the United States Government or any agency thereof. The views and opinions of authors expressed herein do not necessarily state or reflect those of the United States Government or any agency thereof.

References

1. Fleckenstein, W. W, Miskimins J. L., Eustes, A. W, Kazemi, H., Hill, T., Mailand, J., Ortiz, S., and King, G., Development of Multi-Stage Fracturing System and Wellbore Tractor to Enable Zonal Isolation During Stimulation and EGS Operations in Horizontal Wellbores, The Geothermal Rising Conference 2021 (GRC), October 3-6, 2021, San Diego, California, USA. GRC Transactions, Vol. 45, 2021
2. Olasolo, P. & Juárez, M.C. & Morales, M.P. & D'Amico, Sebastiano & Liarte, I.A.. (2016). Enhanced geothermal systems (EGS): A review. Renewable and Sustainable Energy Reviews. 56. 133-144. 10.1016/j.rser.2015.11.031.
3. Eustes, A., Tutuncu, A., Baker, R., Hu, X., Olson, J., Application of horizontal well completion techniques to enhanced geothermal systems: Final Report: October 2015 — September 2016. Golden, CO: National Renewable Energy Laboratory. NREL/SR-6A20-71201, 2018.
4. Gradl, C. and Christian. “Review of Recent Unconventional Completion Innovations and their Applicability to EGS Wells.” (2018). PROCEEDINGS, 43rd Workshop on Geothermal Reservoir Engineering Stanford University, Stanford, California, February 12-14, 2018, SGP-TR-213
5. Guinot, Frédéric , and Peter Meier. "Can Unconventional Completion Systems Revolutionise EGS? A Critical Technology Review." Paper presented at the SPE Europec featured at 81st EAGE Conference and Exhibition, London, England, UK, June 2019. doi: https://doi.org/10.2118/195523-MS
6. Norbeck, J & Latimer, T, U.S. Patent Application 2020/0217181, 2019
7. FORGE 58-32 Injection and Packer Performance – April 2019 FORGE 58-32 packer failure summary.pdf (openei.org)
8. Rytlewski, G. L., & Cook, J. M. (2006, January 1). A Study of Fracture Initiation Pressures in Cemented Cased-Hole Wells Without Perforations. Society of Petroleum Engineers. doi:10.2118/100572-MS

9. Stegent, N. A., Ferguson, K., & Spencer, J. (2011, January 1). Comparison of Frac Valves vs. Plug-and-Perf Completion in the Oil Segment of the Eagle Ford Shale: A Case Study. Society of Petroleum Engineers. doi:10.2118/148642-MS
10. Haustveit, K., Elliott, B., Haffener, J., Ketter, C., O'Brien, J., Almasoodi, M., Deeg, W., Monitoring the pulse of a well through sealed wellbore pressure monitoring, a breakthrough diagnostic with a multi-basin case study. Society of Petroleum Engineers, 2020, doi:10.2118/199731-MS.
11. Alice et al.: Thermal profile and temperature gradients in FORGE Well 58-32, GRC Transactions, Vol. 42. 2018
12. Amini et al.: A three-dimensional thermal model for hydraulic fracturing. SPE ATCE, SPE-174858-MS. 2015
13. Eickmeier et al.: Wellbore temperature and heat losses during production or injection operations. Journal of Canadian Petroleum Technology, April-June Ed., 1970
14. England, K. and McLennan, J.: End of job report, hydraulic fracturing of Well 16A(78)-32, April 2022, Utah FORGE.
15. Fleckenstein et al: Development of multi-stage fracturing system and wellbore tractor to enable zonal Isolation during stimulation and EGS operations in horizontal wellbores, GRC Transactions, Vol. 45, 2021
16. Guinot F and Meier P: Can unconventional completion systems revolutionize EGS? A critical technology review. SPE-195523-MS. 2019
17. Kumar A and Sharma M M: Diagnosing hydraulic fracture geometry, complexity, and fracture wellbore connectivity using chemical tracer flowback. 2018
18. Nadimi et al: DFIT and fracture modeling of the Utah FORGE site. GRC Transactions, Vol. 42, 2018
19. Nadimi et al.: Hydrogeothermal modeling of a granitic based discrete fracture network. Geothermics 87. 2020
20. Ramey H. J., Jr.: Wellbore heat transmission. Journal of petroleum technology, 1962.
21. Simmons et al: Interpretation of hydrothermal conditions, production-injection induced effects, and evidence for enhanced geothermal system-type heat exchange in response to > 30 years of production at Roosevelt Hot Springs, Utah, USA. Geosphere v. 17, no. 6., 2021
22. Simmons, S.F., Kirby, S., Bartley, J., Allis, R., Kleber, E., Knudsen, T., Miller, J., Hardwick, C., Rahilly, K., Fischer, T., Jones, C., and Moore, J. 2019. Update on the Geoscientific Understanding of the Utah FORGE Site. Presented at the 4th Workshop on Geothermal Reservoir Engineering Stanford University, Stanford, California. SGP-TR-214
23. Uzun et al.: Phase behavior change due to rock deformation in shale reservoirs: a compositional approach. SPE-187442-MS, 2017
24. Xing P et al.: In-situ stresses and fractures inferred from image logs at Utah FORGE. 2022
25. Zheng R et al: Heat extraction performance of a downhole coaxial heat exchanger geothermal system by considering fluid flow in the reservoir. 2018
26. Eker et al: Numerical Simulation of Dual-Porosity Multiphase Flow Using Poroelasticity Theory. SPE 182728-MS
27. Nadimi, S., Forbes, B., Moore, J., Podgorney, R., & McLennan, J. D. (2020). Utah FORGE: Hydrogeothermal modeling of a granitic based discrete fracture network. Geothermics, 87, 101853. https://doi.org/https://doi.org/10.1016/j.geothermics.2020.101853

28. Xing, P., McLennan, J., & Moore, J. (2020). In-Situ Stress Measurements at the Utah Frontier Observatory for Research in Geothermal Energy (FORGE) Site. Energies, 13(21). https://doi.org/10.3390/en13215842